THE ASTROPHYSICAL JOURNAL, 244: 903–911, 1981 March 15

THE PECULIAR PLANETARY NEBULA ABELL 35

GEORGE H. JACOBY[1]
Kitt Peak National Observatory[2]
Received 1980 July 14; accepted 1980 September 25

ABSTRACT

The planetary nebula Abell 35 appears strikingly different when photographed in [O III] as compared to its Hα image. The disparity is believed to be due to the effects of a stellar wind originating with a binary central star interacting with the nebular shell. The previously unidentified central star is shown to have a transverse velocity of 150 km s^{-1} and exhibits a wind having a terminal velocity of 185 km s^{-1} at a mass-loss rate of 3×10^{-9} M$_{\odot}$ yr^{-1}. The distance to the nebula is 360 pc, as determined photometrically from the visible member of the binary nucleus.

Subject headings: nebulae: individual — nebulae: planetary — stars: binaries — stars: winds

I. INTRODUCTION

Planetary nebula 35 in Abell's (1966) list of low surface brightness nebulae was first identified on the Palomar Observatory Sky Survey (POSS) plates. It is described as a "homogeneous disk with marked deviation from perfect regularity." The nebula is very large in angular extent, having major and minor axes of 938″ and 636″, respectively. The morphology on the POSS plates is dominated by two parallel linear features about 3′ south of the geometric center of the nebula oriented from northeast to southwest (see Fig. 1*a*).

Abell estimated that the distance to the nebula is 240 pc based on the flux in the Hα+[N II] lines, but was unable to correct this value for the effects of interstellar absorption. Milne (1979) measured the 5 GHz radio flux from Abell 35 and determined the color excess to be $E(B-V)=0.8$. He expresses concern that the extinction is so large for a nearby nebula, but if this value is accepted, it places Abell 35 at a distance of 208 pc as determined from its radio flux, according to the procedure outlined by Milne and Aller (1975). Despite this proximity, no central star has been identified even though a very faint central star should be visible on the POSS plates. An independent estimate of the reddening and distance will be presented in § V, and a variety of problems relating to the central star will be discussed throughout this paper.

Except for radial velocity (-5.8 km s^{-1}) and expansion velocity (4.2 km s^{-1}) measurements by Bohuski and Smith (1974) and photoelectric photometry in the brighter emission lines by Kaler (1980), this planetary nebula has received little attention. Because the low surface brightness Abell planetary nebulae are especially good targets for the photographic camera used in a recent survey of planetary nebulae (Jacoby 1979), Abell 35 was included in the list of program objects. The photograph taken in [O III] λ5007 (see Fig. 1*b*) raised several questions regarding morphology (§ II), ionization sources (§ III), and the nature of Abell 35 (§ IV). An attempt to answer these questions is presented in § VI.

II. MORPHOLOGY

A series of plates was taken of Abell 35 during the spring of 1979 in the light of Hα and [O III] λ5007 using the Kitt Peak National Observatory (KPNO) No. 1 0.9 m telescope with the Carnegie image-tube camera. The Hα image is essentially identical to the POSS plate shown in Figure 1*a* (Plate 12). Figure 1*b* is a 1 hour exposure taken through a 5007 Å interference filter having a 20 Å bandpass. Although deeper plates at this wavelength were subsequently obtained, this exposure benefited from superior seeing.

It is not unusual for planetary nebulae to offer a variety of appearances depending on the viewing wavelength, but the situation for Abell 35 seems extreme. The obvious discrepancy between the two images is the presence of a parabolic region of enhanced [O III] emission which is completely absent at Hα. The bright star near the apex of the parabola (BD $-22°3467$) is surrounded by a cavity where the [O III] emission is very faint. The overall first impression is that of a bow shock reminiscent of the structures described by Gull and Sofia (1979) for LL Ori and ζ Oph, but much more prominent. Those structures were interpreted as distorted interstellar bubbles (Weaver *et al.* 1977) in which a strong stellar wind interacts with streaming interstel-

[1]Visiting Astronomer, Cerro Tololo Inter-American Observatory, supported by the National Science Foundation under contract AST 74-04128.

[2]Operated by the Association of Universities for Research in Astronomy, Inc., under contract with the National Science Foundation.

lar gas. An interpretation of Abell 35 as a distorted bubble will be presented in § VI. An objection to this treatment is that BD $-22°3467$ has a spectral class (G8 IV; see § V*a*) not generally associated with stars producing strong winds (Sanner 1976). Further, the region of enhanced emission is seen only in [O III], whereas the bubbles observed by Gull and Sofia exhibit enhancements in the Balmer lines as well, though weakly in the case of ζ Oph. Thus the bubble model would seem to be less appropriate here. This topic will be explored further in § VI.

III. IONIZATION SOURCES

Because Abell 35 radiates energy in emission lines characteristic of ionized atoms, an energy source must be present or the nebula would recombine to a neutral state within a few thousand years. Although this time scale is sufficiently long so that ionization equilibrium is not a necessary condition, it is usually assumed to be the case.

The nebula can be treated as a two-component system with one component being the overall spherical nebula and the second component consisting of the region directly affected by the bow wave phenomenon. We consider first the problems associated with ionizing the main nebula.

Abell (1966) did not identify a central star in this nebula because there are no blue stars in the field near the nebula center. This is by no means unusual; 19 of the 84 planetary nebulae in Abell's list do not have an associated central star. In most cases, this can be attributed to the greater distances (2–4 kpc) involved, but a few nebulae (numbers 38, 56, and 62) are genuinely lacking identifiable central stars.

We can estimate the visual magnitude for a central star in Abell 35 by reversing the Zanstra temperature procedure. An approximate Hβ flux is given by Kaler (1980) as $\log F(\mathrm{H}\beta) = -11.3$ in cgs units. The stellar temperature can be assumed for the moment to be greater than 50,000 K in order that oxygen be doubly ionized. Then the V magnitude must be less than about 16.6. The star could be brighter than this because the nebula is optically thin so that the Hβ flux represents a lower limit to the ultraviolet photon flux assumed. On the other hand, the temperature could be higher than that assumed, resulting in a smaller visible flux for the same ultraviolet flux. Also, the observed magnitude may be fainter if the interstellar extinction is as great as found by Milne (1979), but the extinction will be shown later to be negligible. Now we have the curious situation in which an adequately bright blue star should be present in the field of Abell 35 but is, in fact, not evident.

Two alternative explanations for the nebula ionization must therefore be considered. First, the bow wave represents a shock emitting sufficient ultraviolet radiation to ionize the entire nebula. Second, the ultraviolet central star is not seen because it is the companion of a brighter star forming a binary (possibly optical) planetary nebula nucleus. The first alternative can be shown to be improbable on the basis of energy requirements. The kinetic energy needed to power the entire nebula is more than an order of magnitude greater than is available (see § VI). More importantly, the second alternative is supported observationally (see § V*a*). We propose then that, in the case of Abell 35, a hot subdwarf central star is present but is masked by the bright star BD $-$ 22°3467 ($V = 9.6$). Central stars having this configuration are unusual but not unprecedented (Lutz 1977).

Now consider the ionization source for the second component in the nebula, the enhanced [O III] region. The λ5007 photograph (Fig. 1*b*) demands that attention be focused near the bright star at the head of the bow wave. This star has a measured proper motion of $0.086 \pm 0.025''$ yr^{-1}, directed at a position angle of 244°.6 (Schlesinger and Barney 1943; Fallon 1979) as indicated by the arrow in Figure 1*b* labeled V_t. The direction of motion is very nearly along the axis of symmetry of the bow wave, and the magnitude of the transverse motion is about 150 km s^{-1} (see § V*a* for the distance determination). If a stellar wind is present, the kinetic energy of the star can be coupled to the nebula to provide a source for the additional energy needed to enhance the ionization level near the star. This mechanism will be discussed in more detail in § VI.

IV. THE NATURE OF THE NEBULA

The limited data previously available concerning Abell 35 raises some doubt as to the validity of its classification as a planetary nebula. Besides the problem of its central star and its unusual morphology, several peculiarities are evident. It is extremely large. Its diameter of 1.6 pc makes it one of the largest planetary nebulae known. It has a small expansion velocity (4.2 km s^{-1}) which may be interpreted as due to deceleration by the surrounding interstellar medium; however, Bohuski and Smith (1974) find this explanation untenable due primarily to the low interstellar medium density. Consequently, the nebula has the very great age of 185,000 years, making it the oldest known planetary nebula. Note, though, that Bohuski and Smith determined the expansion velocity only from the [O III] line and only within an aperture (120″) much smaller than the nebular diameter (938″).

Abell 35 also has a moderate height above the galactic plane (230 pc) which is not unusual but does exceed the more typical values of $\sim$150 pc (Osterbrock 1974). Its shell mass is not unusual (0.2 $M_\odot$), as found by inverting the Shklovskii method (Aller and Liller 1968) of distance determination.

Therefore, it seems reasonable to question the classification of Abell 35. However, its characteristics do not match any other class of object any better, so the following discussions will be based on the assumption that Abell 35 is a very old planetary nebula. We can then proceed to attempt to understand the mechanism responsible for the unusual morphology.

V. OBSERVATIONS

The photographic observations which caused the concerns outlined in the previous sections have already been presented. It was clear at the outset that additional data would be needed to interpret the photograph in a consistent fashion. The following observations were subsequently secured.

a) *Photometry*

DDO and *UBVRI* photometry of BD $-22°3467$ was obtained on 1980 February 22 and 23 at the CTIO No. 1 0.4 m telescope. The purpose of the photometry was to obtain an accurate spectral class, extinction, metallicity, and apparent magnitude for the star at the head of the bow wave. Additionally, a primary goal was to test for an ultraviolet companion by examining the stellar colors.

Eighteen DDO standards were chosen from the equatorial group given by McClure (1976) and 17 *UBVRI* standards were chosen from the equatorial sequences of Moffett and Barnes (1979). Although a red star a few seconds of arc to the south was included in the 18″ aperture, it is several magnitudes fainter than BD $-22°3467$ and does not contaminate the blue photometry. The data was transformed to the standard set in the usual fashion, and no observations with air masses greater than 1.5 were used.

The derived colors are given in Table 1, along with one standard deviation uncertainties derived from multiple measurements during each night. These uncertainties are similar to the deviations of the observed colors of the standards from their published values and are probably representative of the true errors.

TABLE 1

PHOTOMETRY FOR BD $-22°3467$

Index	Magnitude	σ	N
V	9.631	0.010	4
$B-V$	0.904	0.006	4
$U-B$	0.349	0.026	3
$V-R$	0.792	0.006	4
$R-I$	0.517	0.007	4
m_{48}	10.040	0.018	5
C(35−38)...	0.896	0.016	6
C(38−41)...	−0.725 (−0.555)[a]	0.017	6
C(41−42)...	0.120 (0.130)	0.016	6
C(42−45)...	0.784 (0.804)	0.012	6
C(45−48)...	1.119 (1.139)	0.012	5

[a]See text for description of values in parentheses.

The spectral class of BD $-22°3467$ is determined from the DDO colors, C(45−48), C(41−42), and C(42−45) (Janes 1975) to be G8 IV. The broad-band indices, $R-I$ and $V-R$, are consistent with this classification, although they indicate the slightly later type K0 IV (Johnson 1966). A spectrum of the star (§ V*b*) favors the earlier type, so the class G8 IV will be adopted temporarily.

The $B-V$ and $U-B$ standard colors for a G8 IV are 0.85 and 0.51, respectively. The star is somewhat bluer than the standard, according to the U magnitude. The excess ultraviolet radiation can be explained in two ways—either the star is very metal deficient or an additional ultraviolet source is present. The former possibility can be tested by examining the DDO CN index δCN (Janes 1975). From Table 1, we see that C(41−42) is 0.120, and from Figure 3 of Janes (1975), the standard C(41−42) is 0.108. The residual, δCN, then is 0.012, corresponding to a metallicity index [Fe/H] of -0.15, or slightly below solar. Thus BD $-22°3467$ is not particularly metal deficient. This conclusion is further supported by the spectrum shown in Figure 2 (see § V*b*), and suggests the presence of a hot compact companion star to supply the ultraviolet excess. Moreover, the resultant contribution to the continuum from the hot companion has led to an improper estimate of the spectral classification for BD $-22°3467$.

If we assume a 50,000 K blackbody companion is responsible for the $U-B$ excess of 0.16 mag, then the U magnitude of the companion will be 13.0. Removing this blackbody flux from the DDO indices results in a revised color set. These colors are included in Table 1 in parentheses and lead to an improved estimate of the spectral class for the visible component as G8 III–IV with [Fe/H]≈ -0.22.

The above correction scheme can be iterated one more time but converges at G8 III–IV with a subdwarf U mag of 12.4. For a very hot blackbody $U-V$ is -1.8 mag, so that V will be 14.2 mag.

The distance to BD $-22°3467$ is obtained photometrically. From an apparent visual magnitude of 9.63 and a typical absolute magnitude of $+1.9$ (Janes 1975, 1979), the distance is 360 pc. The uncertainty in the luminosity class and calibration of the absolute magnitude is estimated at 0.5 mag (Yoss, Karman, and Hartkopf 1980). Thus, the distance uncertainty is 80 pc. No correction is applied for interstellar extinction as there is no evidence in the colors for the presence of any reddening. Rather, it is clear that the color excess of $E(B-V)=0.8$ found by Milne (1979) must be spurious or the $(B-V)_0$ would be unacceptably blue. Additional evidence for a low color excess is found by Cleary, Heiles, and Haslam (1979) from H I maps of the Galaxy showing that the maximum $E(B-V)$ in the direction of Abell 35 is 0.10 mag.

b) *Stellar Spectroscopy*

A widened spectrum of BD $-22°3467$ was obtained at the KPNO No. 1 0.9 m telescope in 1979 July. Using the White spectrograph and image-tube camera at a reciprocal dispersion of 47 Å mm^{-1}, the spectrum has a resolution of 1.2 Å. This spectrum was intended to be used for spectral classification, but, due to poor conditions, an insufficient number of spectral standards were observed. Nevertheless, the spectrum, shown in Figure 2, is consistent with the G8 III–IV classification and shows the star to have normal metallicity.

c) *Spectrophotometry*

In 1980 February, spectra at four positions in the nebula were obtained at the CTIO 1.5 m telescope with the SIT vidicon spectrograph. The slit dimensions were chosen to be 2″ in width by 5.′5 in length. Thirty-minute exposures were taken at positions 13″ north and 8″, 20″, and 120″ south of BD $-22°3467$. The center of the slit was maintained along a north-south line approximately midway between BD $-22°3467$ and the moderately bright star 2.′5 east. The spectra cover the range from 3650 Å to 5100 Å.

The data were reduced using the standard routines provided by the CTIO reduction system. Because information along the slit is required for the study of the spatial variations in the nebula, the two-dimensional spectral image (512 points by 140 lines) from the vidicon was corrected for deviations from a flat field. This was accomplished by dividing all frames by a smoothed scan of the twilight sky with the solar spectrum removed. The system sensitivity was determined by referencing observations to the southern standard, W485, which was observed immediately before and after the observations of Abell 35.

Because the nebula is larger than the longest available slit length, simultaneous observations of the sky could not be made. Therefore, the resulting spectra are not sky subtracted. However, this is of little consequence to the net emission-line strengths, with the possible exception of the temperature dependent line of [O III] λ4363. This line is contaminated by the mercury line at 4358 Å emitted by the streetlights of nearby towns. Although the mercury line is generally considered to be absent at CTIO, it is definitely visible on several of the higher resolution photographic spectra (see below). It is, however, extremely faint as is λ4363 so that the measured strength of λ4363 will provide an upper limit to the computed nebular temperatures.

As Abell 35 has a very low surface brightness, the data were summed along the slit for 12 positions with each position subtending 26″ (11 lines). Still the only emission lines which could be measured reliably were [O II] λ3727, Hγ λ4340, Hβ λ4861, and [O III] λλ4959, 5007. For most positions in the nebula, [O III] λ4363 is measurable, and in several positions, [Ne III] λ3868 is measurable. Table 2 summarizes the line fluxes. The absolute flux is given for λ5007 which is generally the highest signal-to-noise line, and line strengths relative to $F(5007)=100$ are tabulated. The upper limit to the

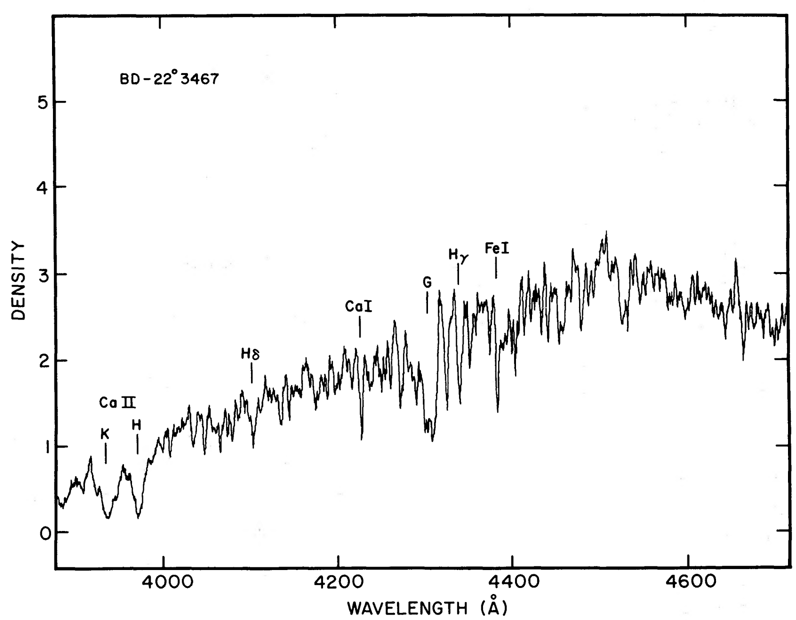

FIG. 2.—A density tracing of the spectrum of BD $-22°3467$

TABLE 2
RELATIVE EMISSION LINE STRENGTHS IN ABELL 35

Position Along Slit[a]	211E	182E	154E	125E	97E	68E	39E	11E	20W	49W	78W	106W
Slit Position[b] 13N												
Line												
3727 [OII]	186	137	102	91	86	85	48	61	39	66	84	82
3868 [NeIII]									5.3	5.9	7.1	5.6
4340 Hγ	9.2	6.9	7.0	9.3		5.8	6.5	4.4		3.1	5.2	2.7
4363 [OIII]	3.4		9.7	2.9		1.4	2.2	4.2	1.7	2.8	4.6	1.9
4861 Hβ	23	21	13	13		8.2	7.3	13	6.3	8.3	7.7	5.3
4959 [OIII]	30	33	39	37	35	32	35	35	29	30	37	31
F(5007)[c]	.223	.294	.344	.353	.321	.353	.415	.395	.718	.482	.434	.418
T_{max}, °K[d]	19400			17700		12700	15400		13700	17300		14400
Slit Position[b] 8S												
3727 [OII]	142	120	75	70	42	39	47	22	31	47	89	80
3868 [NeIII]	6.5		3.9	9.9	5.0	1.8	2.2	3.2	2.7	4.5	4.6	
4340 Hγ	6.1		7.1		5.6	2.4	3.4	8.3	3.4	3.3	5.9	5.0
4363 [OIII]	5.2		1.9		2.7	3.3	1.6	6.2	2.9	2.0	4.3	2.4
4861 Hβ	16	13	10	8.3	7.9	8.2	5.7	6.3	4.9	5.8	5.2	9.8
4959 [OIII]	41	34	34	33	35	29	31	31	29	33	25	31
F(5007)	.260	.306	.446	.476	.537	.579	.596	.495	.952	.530	.401	.390
T_{max}[d]			14400		17000	19000	13400		17700	14700		16000
Slit Position[b] 20S												
3727 [OII]	137			77	37	40	48	23	30	45	83	76
3868 [NeIII]				4.3	2.4	3.7	2.0	3.3	6.2	3.1		3.5
4340 Hγ	10					4.6	10.3	10.2	4.0	6.9	2.8	
4363 [OIII]	5.9					4.2	1.5	7.1	2.9	2.7		
4861 Hβ	22			12	5.0	5.4	11.1	9.5	4.6	12	12	11
4959 [OIII]	46			31	35	26	26	34	39	32	38	27
F(5007)	.215			.503	.586	.634	.636	.760	.971	.625	.434	.439
T_{max}[d]							13100		17700	17000		
Slit Position[b] 120S												
3727 [OII]	486	269	249	199	147	143	133	119	143	125	131	123
3868 [NeIII]		9.0	7.2	4.1	4.1	0.4	1.0	2.1	6.0	2.5	5.2	2.8
4340 Hγ	25	7.5	16	7.6	3.9	5.3	7.4	5.4	9.0	5.9	7.1	
4363 [OIII]	6.0	3.6	4.8	3.2	1.4	1.5	1.1	2.2			1.6	
4861 Hβ	41	31	19	20	11	19	14	18	18	14	14	12
4959 [OIII]		32	44	38	36	28	29	36	35	21	33	30
F(5007)	.138	.231	.225	.277	.357	.415	.509	.587	.603	.433	.368	.375
T_{max}[d]		20200		18700	12700	13100	11700	15400			13400	

[a]Angular distance to BD −22°3467 in arcsec, from the east to west limits of the slit.
[b]Angular distance (arcsec) of slit north or south of BD −22°3467.
[c]In ergs cm^{-2} $s^{-1} \times 10^{13}$.
[d]Upper limit of the electron temperature as derived from the ratio of $I(4363)/I(5007)$.

temperature as derived from the [O III] line ratio $I(4363)/I(5007)$ is also included. The effects of interstellar reddening are negligible and no correction has been applied. The values in the table are only approximate for values smaller than 5 and may be in error by a factor of 2. Values greater than 25 should be accurate to better than 20%.

The derived temperatures extend from about 12,000 K to greater than 20,000 K. We can also derive the abundance of oxygen relative to hydrogen in the usual way. Because no ionization correction can be made for neutral oxygen or ionization levels higher than O III, the derived abundance will be a lower limit. However, in positions where [O II] is weak, this effect is small. Then we have $N(\mathrm{O})/N(\mathrm{H}) \gtrsim 0.0003$.

Kaler (1980) measured the line intensity for [N II] relative to Hβ as 2.2 at a position 3′ south of BD $-22°3467$. The SIT data nearest this position indicate a temperature of 15,400 K. The singly ionized nitrogen abundance, $N(\mathrm{N+})/N(\mathrm{H+})$, is then 1.6×10^{-5}. Although this is perhaps a factor of 5 below typical planetary nebula values for $N(\mathrm{N})/N(\mathrm{H})$ (Aller 1978), no ionization correction factor has been applied either.

Figure 3 shows a series of 12 scans which exemplify the SIT data. Each scan is plotted to the same scale and moves along the slit from east (top) to west (bottom) at the 13″ north position. The trend is evident—as the [O II] intensity decreases near the bow wave, the [O III] intensity increases. As the relative ionic concentration, $N(\mathrm{O}^+)/N(\mathrm{O}^{++})$, is nearly proportional to $I(3727)/I(5007)$, the appearance of the bow wave is seen to be the result of the change in ion populations. Note that the Hβ intensity remains fairly constant, as would be expected from inspection of the POSS plate. If, however, the bow wave were due to a shock, the Balmer line intensities would increase as the square of the density enhancement. Apparently there is no strong density increase.

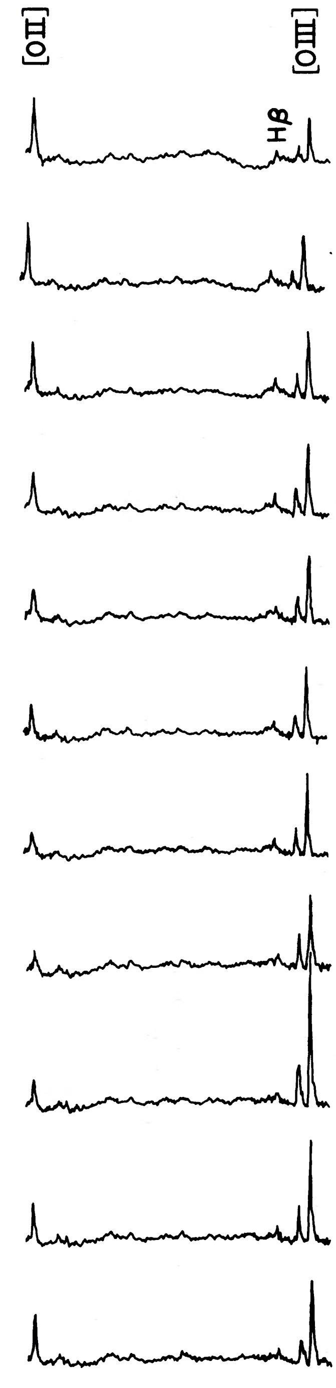

FIG. 3.—A series of SIT vidicon scans of Abell 35 at a position 13″ north of BD $-22°3467$. Each scan is a sum along 26″ of a 2″ wide slit. The scans proceed from east (top) to west (bottom). Note the relative behavior of the lines of [O II] λ3727 and [O III] λ5007 as a function of position. The ninth scan is nearest the bow wave seen in Fig. 1*b*.

d) *Nebular Spectroscopy*

Intermediate resolution (1 Å) spectra of the nebula in three of the four SIT positions (13″ north, and 8″ and 120″ south) were obtained with the CTIO Yale 1 m telescope and image-tube spectrograph on 1980 February 25. Exposures of 90 minutes were taken in the blue to derive the density dependent line ratio of [O II], $I(3729)/I(3726)$. The length of the slit was 3′.7 and the width was 4″. The doublet is cleanly separated and the intensities along the slit are calculated from the photographic densities via spot sensitometer plates. A check on the density-to-intensity conversion is provided by the null result—the line ratio is nearly constant along the slit and has the value of 1.5 corresponding to the low density limit. Thus, the density in the nebula is less than about 100 cm^{-3}.

The average density also can be computed from the Hα emissivity and the received flux, and the radius and distance of the nebula. Then

$$Ne^2 = \frac{F(\mathrm{H}\alpha)}{4.2\times 10^{-22}\varepsilon d\Theta^2},$$

where Ne is the electron density, $F(\mathrm{H}\alpha)$ is the flux in Hα received at the top of the Earth's atmosphere in ergs cm^{-2} s^{-1}, ε is the volume filling factor (taken here as 1.0), d is the distance to the nebula in parsecs, and Θ is the angular radius of the nebula. For Abell 35, $\langle Ne \rangle$ is then 11 cm^{-3}, which is consistent with the limit derived spectroscopically.

Examination of the plates reveals the presence of the mercury lines at λ4358. Because the resolution of the SIT (9 Å) is significantly lower than that of the plates, the oxygen line at 4363 Å is seriously blended with the sky line in the SIT data. The relative strengths of the two lines are comparable, but the mercury line is clearly variable from exposure to exposure. Therefore, no correction can be easily applied to the spectrophotometric data, and the temperatures given in Table 2 remain as upper limits, and the abundances as lower limits.

Although not intended for radial velocity determinations, the photographic spectra were used to check the nebular velocity because that given by Bohuski and Smith (1974) has an ambiguity of ± 154 km s^{-1}. The result found here, -16 ± 14 km s^{-1}, is consistent with that given earlier by Bohuski and Smith of -5.8 km s^{-1}.

VI. DISCUSSION

The interaction of high-velocity planetary nebulae with the interstellar medium has been considered by Smith (1976) and Isaacman (1979). Discussions by Rasiwala (1969) and Weaver *et al.* (1977) are also applicable.

Smith (1976) surveyed several of the nearby large Abell planetary nebulae for evidence of geometric offset of the central stars but did not find any convincing candidates. Smith recognized the possibility for deselection of nebulae with large offsets due to Abell's criteria for central star identification which requires the central star to be approximately centered. It would seem that Abell 35, a truly good candidate with $\Delta R/R \sim 0.15\pm 0.05$, escaped notice because the central star was not identified, perhaps partly due to the large offset. Note that the offset is not apparent in Figure 1*a* since it is an enlargement of the central region of the nebula. The value for $\Delta R/R$ was obtained by examination of the original POSS prints but is approximate due to the very low surface brightness of the nebula. Nevertheless, an offset in the direction of motion (see Fig. 1*b*) is clearly visible.

Further, as shown by Isaacman (1979), Smith's analysis should include the effects of the stellar wind required by the planetary nebula dynamical models (Mathews 1966) and observed in several nebulae (Heap 1979). Isaacman concludes that for solar neighborhood planetary nebulae, the time required to stop the leading edge of the nebula with respect to the central star would be on the order of the lifetime of the nebula and, hence, such nebulae would not be observable. But in the case of Abell 35, a variety of extreme properties conspire to allow this deceleration to take place during the visible lifetime of the nebula. The slow expansion velocity significantly extends the nebular lifetime, while its high velocity relative to the interstellar medium reduces the time for an observable offset. Additionally, the motion of the nebula is very nearly in the plane of the sky ($i<5°$), so that the bow wave is maximally observable. Therefore, it becomes possible to see a planetary nebula with the characteristics of a distorted interstellar bubble as described by Weaver *et al.* (1977).

For a star ejecting mass at a time averaged rate $\dot{m}$ and terminal velocity v_w and moving with respect to the surrounding medium at a velocity v, the wind is in dynamic equilibrium when

$$\dot{m}v_w = 4\pi r_{\min}^2 \rho v^2, \tag{1}$$

where $r_{\min}$ is the minimum distance from the star to the leading edge of the bow wave, and ρ is the density of the medium. In this case, ρ is the density of the undisturbed planetary nebula.

The shape of the bow wave is a paraboloid of revolution (Weaver *et al.* 1977) in which the distance behind the wave and along the axis, z, is related to the perpendicular distance, y, by

$$y^2 = \left(\frac{20L_w}{33\pi\rho v^3}\right)^{1/2} z, \tag{2}$$

where L_w is the power in the stellar wind defined as

$$L_w = \tfrac{1}{2}\dot{m}v_w^2. \tag{3}$$

As suggested in § III and § V*b*, the bow wave appears to be prominent in [O III] due to a change in ionization levels. If the entire energy of the wind is utilized only to ionize the O$^+$–O^{++}, we have that

$$L_w = I_p(\mathrm{O}^+)\frac{N(\mathrm{O}^+)}{N(\mathrm{H}^+)}\frac{\chi M_{\mathrm{neb}}}{m_{\mathrm{H}}}\frac{1}{\tau_r(\mathrm{O}^+)}, \tag{4}$$

where $I_p(\mathrm{O}^+)$ is the ionization potential required to doubly ionize O$^+$ and $N(\mathrm{O}^+)/N(\mathrm{H}^+)$ is the fraction of O$^+$ atoms relative to H$^+$. The mass of the nebula, M_{neb}, is modified by the volume factor, χ, which represents the fraction of the nebula involved in the phenomenon, and m_H is the mass of the hydrogen atom. The recombination time for O^{++}, τ_r, is found from Aldrovandi and Pequignot (1973) to be

$$\tau_r = \frac{5.4\times 10^{11}}{Ne} \text{ (seconds)}, \tag{5}$$

where Ne is ρ/m_H. Note that equation (4) is subject to the inequality that

$$\tfrac{1}{2} m_H v_w^2 > I_p(O^+), \tag{6}$$

in order that the ionization occur. Equation (4) is approximate because atoms other than oxygen will also be ionized, thereby claiming some of the wind's luminosity. An additional uncertainty is introduced if χ is estimated; alternatively, χ can be computed from equation (4) if the nebular density can be established. The latter procedure will be used here. More importantly, as the bulk of the wind's energy is directed toward heating the gas and not toward ionizing oxygen, equation (4) is actually an inequality with the left-hand side greater than the right-hand side.

Because the thickness of the enhanced O^{++} region, Δr, depends on the recombination time, τ_r, for the case of an infinitesimally thin ionization boundary, we have in the equilibrium condition that

$$\tau_r = \Delta r/v, \tag{7}$$

where Δr is measured from the leading edge of the bow wave.

Having found the distance to the nebula to be 360 pc, and determining the value of the radicand in equation (2) by a least-squares solution to the geometry in Figure 1b, we can solve relations (1)—(7) for v, v_w, $\dot{m}$, and χ. We then have that:

$$v = 14 \text{ km s}^{-1}, \tag{8}$$

$$v_w = 185 \text{ km s}^{-1}, \tag{9}$$

$$\dot{m} = 3\times 10^{-9} M_\odot \text{ yr}^{-1}, \tag{10}$$

$$\chi < 0.4, \tag{11}$$

and

$$L_w = 3.4\times 10^{31} \text{ ergs s}^{-1}. \tag{12}$$

From equation (8) we see that the nebula has been slowed significantly with respect to the star by the interstellar medium. In fact, the star is now traveling through the nebula at nearly Mach 1.5, as the sound speed in the ionized gas is about 11 km s^{-1}. The time required to decelerate the nebula can be approximated by treating the nebula as a sphere whose motion is retarded by the dynamic pressure from the interstellar medium. Then the deceleration will be

$$\frac{dv}{dt} = \frac{1}{M_{\rm neb}}\left(\frac{1}{2}\rho_{\rm ism} v_{\rm neb}^2\right)(\pi R^2), \tag{13}$$

where $\rho_{\rm ism}$ is the density of the interstellar medium, and R is the radius of the nebula. Then for $dv = 14$ km s^{-1}, we find that $dt = 55{,}000$ years, if $\rho_{\rm ism}$ is 0.1 cm^{-3}. This is much shorter than the estimated lifetime of the nebula, thereby justifying the implicit assumption of constant nebular radius during the deceleration period. If, in fact, the deceleration is properly characterized by these parameters, then the central star offset, $\Delta R/R$, will be 0.47, which is about 3 times that observed, suggesting that $\rho_{\rm ism} \sim 0.3$ cm^{-3}.

The wind velocity and mass-loss rate (eqs. [9] and [10]) would seem to be excessive for a star of spectral class G8 III–IV (Sanner 1976). Typical mass-loss rates are about less than 10^{-9} $M_\odot$ yr^{-1} and wind velocities are expected to be on the order of several tens of km s^{-1}, but neither of these values is especially well determined. Gull and Sofia (1979) find, for example, that the K0:e star, LL Ori, has a mass-loss rate of $1.5\times 10^{-8} M_\odot$ yr^{-1} and a wind velocity of 600 km s^{-1}, both values exceeding those derived here. Note also that Linsky and Haisch (1979) find the dividing line between weak and strong wind stars to be near spectral class K0.

Alternatively, the postulated unseen companion can radically change the conditions near the giant or is perhaps the sole source of the wind. This possibility is suggested by the *IUE* spectra presented by Heap (1979) showing planetary nebula central stars which produce winds having terminal velocities in excess of 2000 km s^{-1}. Although the derived wind parameters can be checked and the source of the wind tested by obtaining high dispersion spectra of BD $-22°3467$ in the Ca II H and K lines, these observations have so far been frustrated by weather conditions.

The calculated value for χ indicates that sufficient luminosity is provided by the wind to further ionize nearly half the singly ionized oxygen in the nebula. However, the bulk of the energy in the wind does not ionize the oxygen directly but rather heats the nebula. Although the measured temperatures in Table 2 do not show any dramatic temperature increase across the bow wave, the wind luminosity contributes only a few percent toward the total nebular luminosity and the temperature rise is not expected to be measurable in the low signal-to-noise data. Moreover, the data has been averaged over 26″ (0.04 pc), thereby reducing the visibility of any small-scale variations.

VII. CONCLUSIONS

The interpretation of the unusual morphology exhibited by Abell 35 as a distorted interstellar bubble provides a consistent view of the phenomenon. In summary, Abell 35 is a high-velocity, high-galactic latitude, rather unusual planetary nebula which formed from a binary central star. Upon encounter with the interstellar medium, the nebula was decelerated with respect to the central star. This condition, when combined with a stellar wind, provided the mechanism for the distorted bubble as outlined by Weaver *et al.* (1977).

The physical parameters of the nebula determined from this study are:

$$d = 360 \pm 80 \text{ pc},$$

$$R = 0.8 \pm 0.2 \text{ pc},$$

$$M_{\text{neb}} = 0.2 \pm 0.1\ M_\odot,$$

$$V_t = 150 \pm 55 \text{ km s}^{-1},$$

$$Te \lesssim 15{,}000 \text{ K},$$

and

$$\langle Ne \rangle = 11 \text{ cm}^{-3}.$$

The surrounding interstellar medium at a height of 230 pc above the galactic plane has been shown to have a density of $\sim 0.3 \text{ cm}^{-3}$.

In addition to the photometric indices given in Table 1, the central star can be ascribed the following properties:

spectral class—G8 III–IV + hot subdwarf

$$\left[\frac{\text{Fe}}{\text{H}}\right] \approx -0.22,$$

$$E(B-V) \approx 0.0,$$

$$\dot{m}_w = 3 \times 10^{-9} M_\odot \text{ yr}^{-1},$$

and

$$v_w = 185 \text{ km s}^{-1}.$$

Abell 35 has presented a rare opportunity to determine the mass-loss rate and wind characteristics of a planetary nebula central star using indirect methods. When ultraviolet spectra of the central star become available, the predicted existence of the subdwarf and the magnitude of the wind can be verified.

One anomaly not addressed by this study is the pair of parallel linear features described in § I and most visible on the POSS photograph. The orientation of these features is again along the proper motion vector of BD $-22°3467$, suggesting a dynamic origin, and perhaps represents an interface between the nebula shell and the interstellar medium.

I would like to thank Dr. C. Christian for providing the photometry reduction programs, and Drs. T. Gull, J. Kaler, and G. Gisler for several very helpful discussions.

REFERENCES

Abell, G. O. 1966, *Ap. J.*, **144**, 259.
Aldrovandi, S. M. V., and Pequignot, D. 1973, *Astr. Ap.* **25**, 137.
Aller, L. H. 1978, in *IAU Symposium 76, Planetary Nebulae Observations and Theory*, ed. Y. Terzian (Dordrecht: Reidel), p. 230.
Aller, L. H., and Liller, W. 1968, in *Nebulae and Interstellar Matter*, ed. B. M. Middlehurst and L. H. Aller (Chicago: University of Chicago Press), p. 483.
Bohuski, T. J., and Smith, M. G. 1974, *Ap. J.*, **193**, 197.
Cleary, M. N., Heiles, C., and Haslam, C. G. T. 1979, *Astr. Ap. Suppl.*, **36**, 95.
Fallon, F. 1979, private communication.
Gull, T. R., and Sofia, S. 1979, *Ap. J.*, **230**, 782.
Heap, S. R. 1979, in *IAU Symposium 83, Mass Loss and Evolution of O-Type Stars*, ed. P. S. Conti and C. W. H. de Loore (Dordrecht: Reidel), p. 99.
Isaacman, R. 1979, *Astr. Ap.*, **77**, 327.
Jacoby, G. H. 1979, *Pub. A.S.P.*, **91**, 754.
Janes, K. A. 1975, *Ap. J. Suppl.*, **29**, 161.
______. 1979, *Ap. J. Suppl.*, **39**, 135.
Johnson, H. L. 1966, *Ann. Rev. Astr. Ap.*, **4**, 193.
Kaler, J. B. 1980, *Ap. J.*, **239**, 78.
Linsky, J. L., and Haisch, B. M. 1979, *Ap. J. (Letters)*, **229**, L27.
Lutz, J. H. 1977, *Astr. Ap.*, **60**, 93.
Mathews, W. G. 1966, *Ap. J.*, **143**, 173.
McClure, R. D. 1976, *A.J.*, **81**, 182.
Milne, D. K. 1979, *Astr. Ap. Suppl.*, **36**, 227.
Milne, D. K., and Aller, L. H. 1975, *Astr. Ap.*, **38**, 183.
Moffett, T. J., and Barnes, T. G. 1979, *A.J.*, **84**, 627.
Osterbrock, D. E. 1974, *Astrophysics of Gaseous Nebulae* (San Francisco: Freeman), p. 222.
Rasiwala, M. 1969, *Astr. Ap.*, **1**, 431.
Sanner, F. 1976, *Ap. J. Suppl.*, **32**, 115.
Schlesinger, F., and Barney, I. 1943, *Trans. Astr. Obs. Yale Univ.*, **14**, 182.
Smith, H. 1976, *M.N.R.A.S.*, **175**, 419.
Weaver, R., McCray, R., Castor, J., Shapiro, P., and Moore, R. 1977, *Ap. J.*, **218**, 377.
Yoss, K. M., Karman, R. A., and Hartkopf, W. I. 1980, preprint.

George H. Jacoby: Kitt Peak National Observatory, 950 North Cherry Avenue, P.O. Box 26732, Tucson, AZ 85726

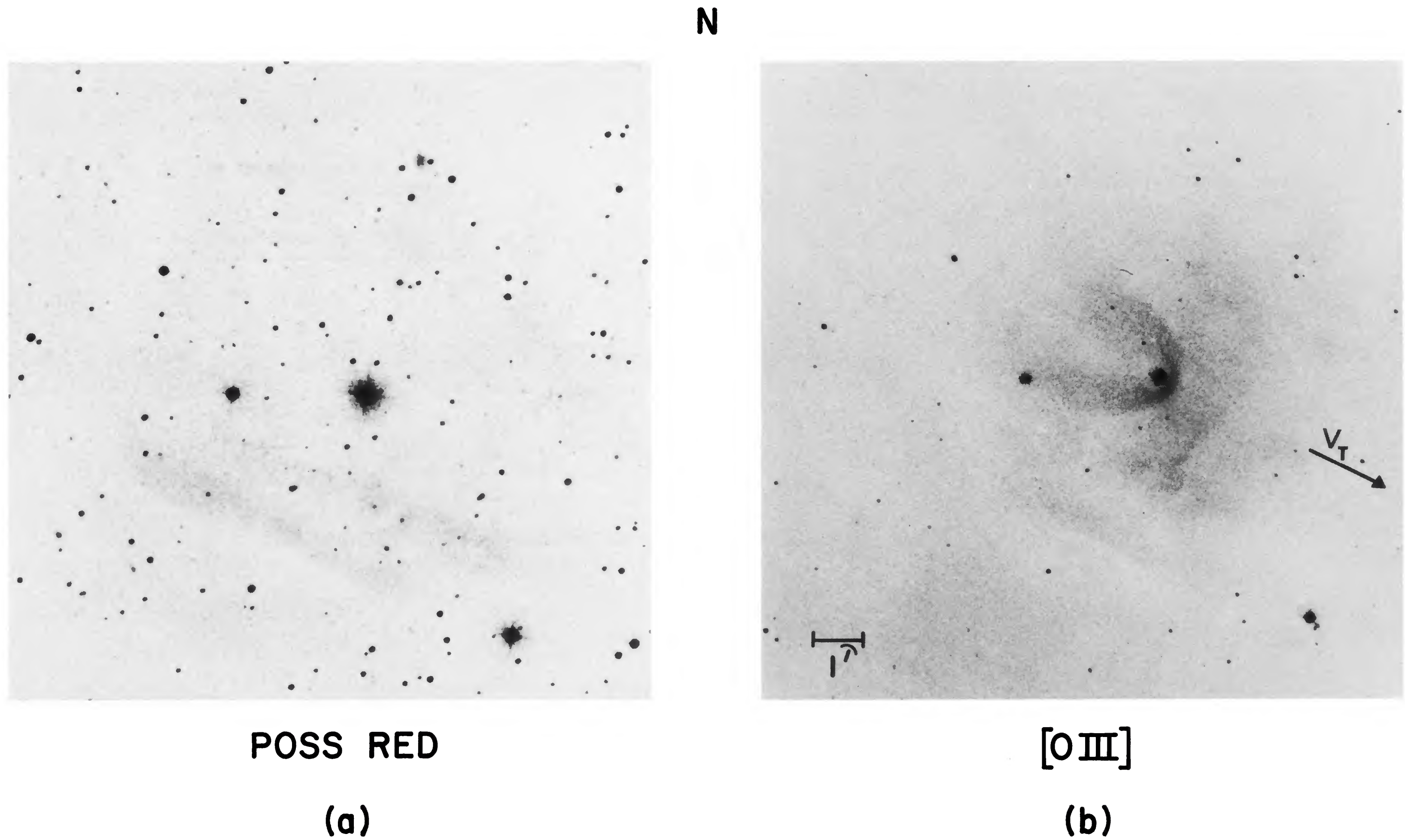

FIG. 1.—Photographs of Abell 35. (*a*) Reproduction from POSS red plate and (*b*) [O III] λ5007 image-tube plate from the KPNO No. 1 0.9 m telescope. The arrow labeled V_t indicates the direction of proper motion for the bright star BD −22°3467.

JACOBY (*see* page 903)